RESEARCH ARTICLES

BLACK HOLE PHYSICS

# Black hole lightning due to particle acceleration at subhorizon scales

J. Aleksić,[1] S. Ansoldi,[2] L. A. Antonelli,[3] P. Antoranz,[4] A. Babic,[5] P. Bangale,[6] J. A. Barrio,[7] J. Becerra González,[8]* W. Bednarek,[9] E. Bernardini,[10] B. Biasuzzi,[2] A. Biland,[11] O. Blanch,[1] S. Bonnefoy,[7] G. Bonnoli,[3] F. Borracci,[6] T. Bretz,[12]† E. Carmona,[13] A. Carosi,[3] P. Colin,[6] E. Colombo,[8] J. L. Contreras,[7] J. Cortina,[1] S. Covino,[3] P. Da Vela,[4] F. Dazzi,[6] A. De Angelis,[2] G. De Caneva,[10] B. De Lotto,[2] E. de Oña Wilhelmi,[14] C. Delgado Mendez,[13] D. Dominis Prester,[5] D. Dorner,[12] M. Doro,[15] S. Einecke,[16] D. Eisenacher,[12]** D. Elsaesser,[12] M. V. Fonseca,[7] L. Font,[17] K. Frantzen,[16] C. Fruck,[6] D. Galindo,[18] R. J. García López,[8] M. Garczarczyk,[10] D. Garrido Terrats,[17] M. Gaug,[17] N. Godinović,[5] A. González Muñoz,[1] S. R. Gozzini,[10] D. Hadasch,[14]‡ Y. Hanabata,[19] M. Hayashida,[19] J. Herrera,[8] D. Hildebrand,[11] J. Hose,[6] D. Hrupec,[5] W. Idec,[9] V. Kadenius,[20] H. Kellermann,[6] K. Kodani,[19] Y. Konno,[19] J. Krause,[6] H. Kubo,[19] J. Kushida,[19] A. La Barbera,[3] D. Lelas,[5] N. Lewandowska,[12] E. Lindfors,[20]§ S. Lombardi,[3] F. Longo,[2] M. López,[7] R. López-Coto,[1] A. López-Oramas,[1] E. Lorenz,[#] I. Lozano,[7] M. Makariev,[21] K. Mallot,[10] G. Maneva,[21] N. Mankuzhiyil,[2]|| K. Mannheim,[12]** L. Maraschi,[3] B. Marcote,[18] M. Mariotti,[15] M. Martínez,[1] D. Mazin,[6] U. Menzel,[6] J. M. Miranda,[4] R. Mirzoyan,[6] A. Moralejo,[1] P. Munar-Adrover,[18] D. Nakajima,[19] A. Niedzwiecki,[9] K. Nilsson,[20]§ K. Nishijima,[19] K. Noda,[6] R. Orito,[19] A. Overkemping,[16] S. Paiano,[15] M. Palatiello,[2] D. Paneque,[6] R. Paoletti,[4] J. M. Paredes,[18] X. Paredes-Fortuny,[18] M. Persic,[2] J. Poutanen,[20] P. G. Prada Moroni,[22] E. Prandini,[11] I. Puljak,[5] R. Reinthal,[20] W. Rhode,[16] M. Ribó,[18] J. Rico,[1] J. Rodriguez Garcia,[6] S. Rügamer,[12] T. Saito,[19] K. Saito,[19] K. Satalecka,[7] V. Scalzotto,[15] V. Scapin,[7] C. Schultz,[15] T. Schweizer,[6] S. N. Shore,[22] A. Sillanpää,[20] J. Sitarek,[1]** I. Snidaric,[5] D. Sobczynska,[9] F. Spanier,[12] V. Stamatescu,[1]¶ A. Stamerra,[3] T. Steinbring,[12] J. Storz,[12] M. Strzys,[6] L. Takalo,[20] H. Takami,[19] F. Tavecchio,[3] P. Temnikov,[21] T. Terzić,[5] D. Tescaro,[8] M. Teshima,[6,19] J. Thaele,[16] O. Tibolla,[12] D. F. Torres,[23] T. Toyama,[6] A. Treves,[24] M. Uellenbeck,[16] P. Vogler,[11] R. Zanin,[18] M. Kadler,[12] R. Schulz,[12,25] E. Ros,[26,27,28] U. Bach,[26] F. Krauß,[12,25] J. Wilms[25]

**Supermassive black holes with masses of millions to billions of solar masses are commonly found in the centers of galaxies. Astronomers seek to image jet formation using radio interferometry but still suffer from insufficient angular resolution. An alternative method to resolve small structures is to measure the time variability of their emission. Here we report on gamma-ray observations of the radio galaxy IC 310 obtained with the MAGIC (Major Atmospheric Gamma-ray Imaging Cherenkov) telescopes, revealing variability with doubling time scales faster than 4.8 min. Causality constrains the size of the emission region to be smaller than 20% of the gravitational radius of its central black hole. We suggest that the emission is associated with pulsar-like particle acceleration by the electric field across a magnetospheric gap at the base of the radio jet.**

More than three decades ago, it was proposed that the radio emission of extragalactic jets results from a relativistically moving plasma consisting of magnetic fields and accelerated particles following a power-law energy distribution (*1*). One of the major assets of the model is that it can explain the nonthermal emission of extragalactic jets across the entire electromagnetic spectrum, from radio waves up to gamma rays. The emission can be understood as synchrotron radiation and inverse Compton scattering (*2*, *3*) due to particles accelerated at shock waves in the jets. The gamma rays can reach very high energies measured in giga–electron volts (1 GeV= $10^9$ eV, corresponding roughly to the rest mass energy equivalent of the proton) and tera–electron volts (1 TeV = $10^{12}$ eV). According to the Blandford-Znajek mechanism, the jets are powered by extracting rotational energy from the black holes, which have acquired angular momentum through the accretion of surrounding gas and black hole mergers (*4*), although so far astrophysical evidence for the role of black hole spin is still lacking (*5*). For a maximally rotating supermassive black hole of mass $M = 10^8 m_8 M_\odot$, where $M_\odot$ denotes one solar mass, the size of the jet formation region should be of the order of its gravitational radius, $r_g = G_N M/c^2 \sim 1.5 \times 10^{11} m_8$ m ($G_N$, gravitational constant; $c^2$, speed of light) and twice this value for a nonrotating Schwarzschild black hole. Astronomical telescopes do not yet provide the angular resolution needed to image structures on this scale. The highest-resolution images of jets obtained with very long baseline radio interferometry show radio-emitting knots traveling down the jets (*6*). Approaching the black hole, the spectra cut off at increasingly higher frequencies due to synchrotron self-absorption. Observations at very high frequencies where the core becomes transparent are needed to zoom into the region where the jets are emerging from. The record holder is a very long baseline radio interferometry observation of the jet of the nearby radio galaxy M87 at a frequency of 230 GHz, resolving a source with a size of 11.0 ± 0.8 gravitational radii (*7*).

## The event horizon light-crossing time

Although direct imaging of the jet formation region has to await better angular resolution, indirect information about its size can be inferred

[1]Institut de Física d'Altes Energies, Campus UAB, E-08193 Bellaterra, Spain. [2]Università di Udine and Istituto Nazionale di Fisica Nucleare (INFN) Trieste, I-33100 Udine, Italy, and Istituto Nazionale di Astrofisica (INAF)-Trieste, I-34127 Trieste, Italy. [3]INAF National Institute for Astrophysics, I-00136 Rome, Italy. [4]Università di Siena and INFN Pisa, I-53100 Siena, Italy. [5]Croatian MAGIC Consortium, Rudjer Boskovic Institute, University of Rijeka and University of Split, HR-10000 Zagreb, Croatia. [6]Max-Planck-Institut für Physik, D-80805 München, Germany. [7]Universidad Complutense, E-28040 Madrid, Spain. [8]Instituto de Astrofísica de Canarias, E-38200 La Laguna, Tenerife, Spain. [9]University of Łódz', PL-90236 Lodz, Poland. [10]Deutsches Elektronen-Synchrotron, D-15738 Zeuthen, Germany. [11]ETH Zurich, CH-8093 Zurich, Switzerland. [12]Universität Würzburg, D-97074 Würzburg, Germany. [13]Centro de Investigaciones Energéticas, Medioambientales y Tecnológicas, E-28040 Madrid, Spain. [14]Institute of Space Sciences, E-08193 Barcelona, Spain. [15]Università di Padova and INFN, I-35131 Padova, Italy. [16]Technische Universität Dortmund, D-44221 Dortmund, Germany. [17]Unitat de Física de les Radiacions, Departament de Física, and Centro de Estudios e Investigación Espaciales-Institut d'Estudis Espacials de Catalunya, Universitat Autònoma de Barcelona, E-08193 Bellaterra, Spain. [18]Universitat de Barcelona, Institut de Ciències del Cosmos, Institut d'Estudis Espacials de Catalunya-Universitat de Barcelona, E-08028 Barcelona, Spain. [19]Japanese MAGIC Consortium, Division of Physics and Astronomy, Kyoto University, Japan. [20]Finnish MAGIC Consortium, Tuorla Observatory, University of Turku and Department of Physics, University of Oulu, Finland. [21]Institute for Nuclear Research and Nuclear Energy, BG-1784 Sofia, Bulgaria. [22]Università di Pisa and INFN Pisa, I-56126 Pisa, Italy. [23]ICREA and Institute of Space Sciences, E-08193 Barcelona, Spain. [24]Università dell'Insubria and INFN Milano Bicocca, Como, I-22100 Como, Italy. [25]Dr. Remeis-Sternwarte Bamberg, Astronomisches Institut der Universität Erlangen-Nürnberg, ECAP, D-96049 Bamberg, Germany. [26]Max-Planck-Institut für Radioastronomie, D-53121 Bonn, Germany. [27]Observatori Astronòmic, Universitat de València, E-46980 Paterna, València, Spain. [28]Departament d'Astronomia i Astrofísica, Universitat de València, E-46100 Burjassot, València, Spain. *Present address: NASA Goddard Space Flight Center, Greenbelt, MD 20771, USA, and Department of Physics and Department of Astronomy, University of Maryland, College Park, MD 20742, USA. †Present address: Ecole Polytechnique Fédérale de Lausanne (EPFL), Lausanne, Switzerland. ‡Present address: Institut für Astro- und Teilchenphysik, Leopold-Franzens-Universität Innsbruck, A-6020 Innsbruck, Austria. §Present address: Finnish Centre for Astronomy with ESO (FINCA), Turku, Finland. ||Present address: Astrophysics Science Division, Bhabha Atomic Research Centre, Mumbai 400085, India. ¶Present address: School of Chemistry and Physics, University of Adelaide, Adelaide 5005, Australia. #Deceased. **Corresponding author. E-mail: deisenacher@astro.uni-wuerzburg.de (D.E.); jsitarek@ifae.es (J.S.), mannheim@astro.uni-wuerzburg.de (K.M.)

from the temporal variability of the emission coming from that region. The observed gamma-ray variability time scales indeed reach down to the event horizon light-crossing time, $\Delta t_{BH} = r_g/c = G_N M/c^3 = 8.3 m_8$ minutes (*8*), vindicating the scenario that the jets originate from the magnetospheres of accreting black holes. An example is the radio galaxy M87 in the Virgo cluster of galaxies (*9*, *10*). This galaxy harbors a central supermassive black hole with the enormous mass of ~$6.4 \times 10^9\ M_\odot$ (*11*). M87 exhibits gamma-ray variability on a time scale of days (*12*), which is consistent with the light-crossing time of the event horizon $\Delta t_{BH}(\mathrm{M87}) = 0.4$ days.

## Smaller than a black hole?

Observations of Mrk 501 (*13*) and PKS 2155-304 (*14*) at very high energies have provided evidence for extreme variability events, with flux doubling time scales as short as ~2 min. The ultrafast variability corresponds to $\Delta t < \Delta t_{BH}$ and therefore casts a shadow of doubt on the current shock-in-jet paradigm. It has been suggested that relativistic bulk motion of the jets could explain the observed time scales (*15*). The argument relies on the observation that these flaring sources belong to the class of sources that astronomers call blazars. In blazars, the jets are pointing at a small angle toward the observer. Because the jet plasma moves with a speed close to the speed of light $\beta = v_j/c \simeq 1$, leading to a bulk Lorentz factor $\Gamma_j > 1$, several effects arise due to the relativistic boosting of the emission (*16*). One of them affects the time scale of flux variations of the emission from a shock. The moving shock plasma almost catches up with its own radiation, and this leads to a shortening of the observed variability time scale $\Delta t$ as compared with the variability time scale $\Delta t'$ in a frame co-moving with the shock given by $\Delta t = (1+z)\delta^{-1}\Delta t'$, where $z$ denotes the cosmological redshift of the source. For a given value of $\Gamma_j$, the Doppler factor $\delta$ depends strongly on the orientation angle of the jet $\theta$ (Fig. 1). Note that $\theta = 0$ corresponds to perfect alignment. For Mrk 501 and PKS 2155-304, almost perfectly aligned jets with $\Gamma_j > 50$ would be needed to accommodate for $\Delta t < \Delta t_{BH}$ and to avoid self-absorption of the gamma rays because of pair production (*15*). In blazars, interferometric observations of the superluminal motion of radio knots suggest lower values of $\Gamma_j$~10 and orientation angles of a few degrees (*17*). Larger values of $\Gamma_j$ would lead to a problem with population statistics: The number of unbeamed counterparts of blazars viewed at larger angles would then exceed the number of radio galaxies, which are commonly believed to represent the misaligned blazars (*18*). Assuming lower black hole masses would bring down $\Delta t_{BH}$. However, lower masses conflict with the firmly established dynamical measurements of black hole masses and therefore do not seem to be a likely solution of the dilemma. Other possible solutions of this Doppler factor crisis (*19*) invoke models of structured jets (*20*, *21*) or Poynting flux–dominated jets, in which only a few but very fast seed particles at the jet base reach high Lorentz factors (*22*–*24*) before the Poynting flux is converted into the kinetic energy of the bulk flow by mass entrainment.

All of these attempts to explain the subhorizon scale variability with relativistic projection effects alone ignore a fundamental problem. If the perturbations giving rise to the blazar variability are injected at the jet base, the time scale of the flux variations in the frame co-moving with the jet is affected by time dilation with Lorentz factor $\Gamma_j$. In blazars where $\delta \sim \Gamma_j$, the Lorentz factor cancels out and the observed variability time scale is ultimately bounded below by $\Delta t_{BH}$.

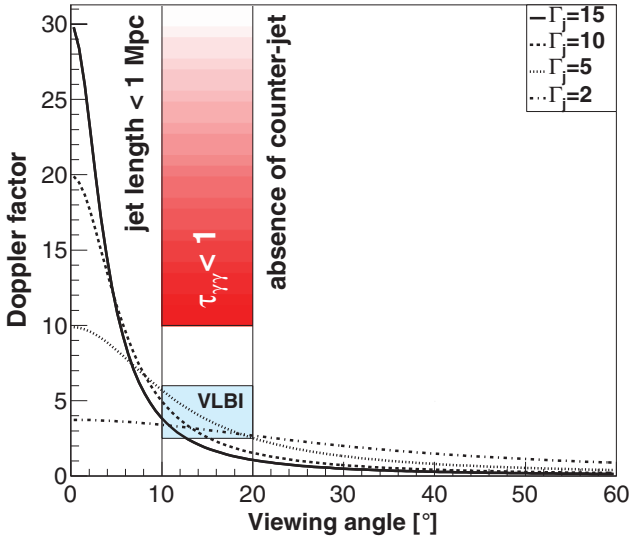


**Fig. 1. The relation between Doppler factor and orientation angle evaluated for various values of the bulk Lorentz factor compared with the observational constraints of these parameters.** The blue box shows the constraints on the Doppler factor arising from radio observations (*32*). For illustrative purposes, the red box shows the constraint from the gamma-ray optical depth to pair creation, assuming $L_{syn} \sim 1\%\ L_{VHE}$.

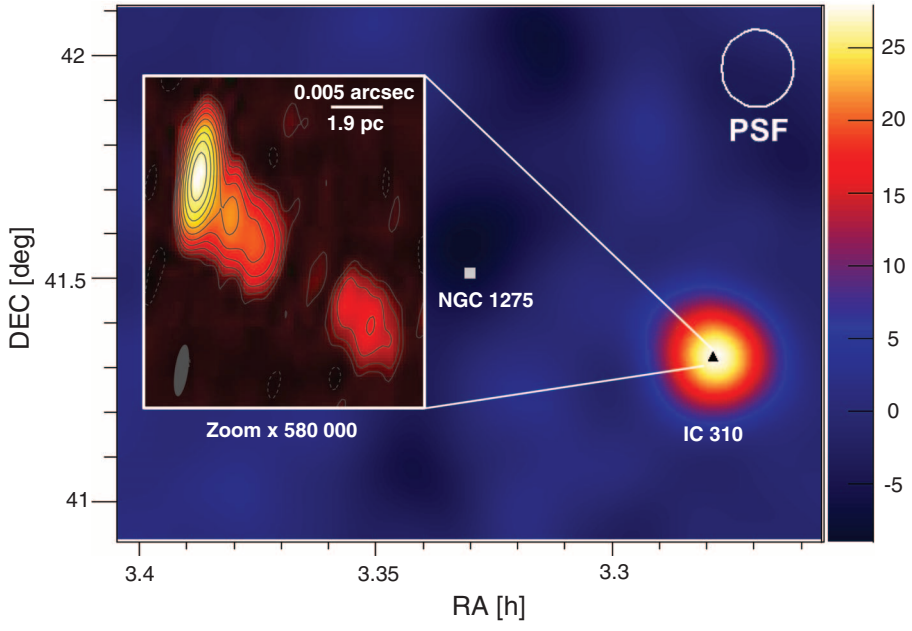


**Fig. 2. Significance map (color scale) of the Perseus cluster in gamma rays observed on the night of 12/13 November 2012 with the MAGIC telescopes.** The inset shows the radio jet image of IC 310 at 5.0 GHz obtained with the European Very Long Baseline Interferometry Network (EVN) on 29 October 2012. Contour lines (and the color scale associated with them) increase logarithmically by factors of 2, starting at three times the noise level (see the supplementary materials for image parameters). The ratio of the angular resolution between MAGIC and the EVN is 1:580 000.

## IC 310: A gamma-ray lightning inferno

IC 310 is a peculiar radio galaxy located in the outskirts of the Perseus cluster at a distance of 260 million light years from Earth. On 12/13 November 2012, MAGIC (Major Atmospheric Gamma-ray Imaging Cherenkov), a system of two Imaging Atmospheric Cherenkov telescopes located on the Canary island of La Palma (*25*), detected an extraordinary outburst of gamma rays from this object (Fig. 2 and fig. S1). The details of the analysis can be found in section S2. Before these observations, variable gamma-ray emission from IC 310 had already been detected by satellite and ground-based gamma-ray instruments at GeV and TeV energies; e.g., Fermi-LAT and MAGIC (*26*–*28*). On the night of the flare in

November 2012, the mean flux above 300 GeV was $(6.08 \pm 0.29) \times 10^{-11}$ cm$^{-2}$s$^{-1}$; that is, four times higher than the highest flux during previous observations in 2009/2010. The measured spectrum (Fig. 3) can be described by a simple power law with a differential photon spectral index of $\Gamma = 1.90 \pm 0.04_{\rm stat} \pm 0.15_{\rm syst}$ in the energy range of 70 GeV to 8.3 TeV (table S2). Owing to its proximity, the spectrum of IC 310 is only marginally affected by photon-photon absorption in collisions with the extragalactic background light (EBL).

IC 310 harbors a supermassive black hole with a mass of $M = (3^{+4}_{-2}) \times 10^8 M_{\rm sun}$ (section S1.1), corresponding to an event horizon light-crossing time of $\Delta t_{\rm BH} = (23^{+34}_{-15})$ min. The mass has been inferred from the correlation of black hole masses with the central velocity dispersion of their surrounding galaxies (*29*, *30*). The reported errors are dominated by the intrinsic scatter of the distribution. The same value of the mass is obtained from the fundamental plane of black hole activity (*31*). The scatter in the fundamental plane for a single measurement is larger and corresponds to a factor of ~7.5.

During 3.7 hours of observations, extreme variability with multiple individual flares was detected (Fig. 4 and figs. S3 and S4). The flare has shown the most rapid flux variations ever observed in extragalactic objects, comparable only to those seen in Mrk 501 and PKS 2155-304. A conservative estimate of the shortest variability time scale in the frame of IC 310 yields $\Delta t/(1+z) = 4.8$ min. It is the largest doubling time scale with which the rapidly rising part of the flare can be fitted with a probability $> 5\%$ (fig. S4). The light curve also shows pronounced large-amplitude flickering characterized by doubling time scales down to $\Delta t$~1 min. The conservative variability time scale corresponds to 20% of the light travel time across the event horizon, or 60% of it, allowing for the scatter in the dynamical black hole mass measurement.

From the absence of a counter radio jet and the requirement that the proper jet length does not exceed the maximum of the distribution of jet lengths in radio galaxies, the orientation angle was found to be in the range $\theta \sim 10°$ to $20°$ (section S1.2), and the Doppler factor consistent with $\delta \approx 4$ (*32*). These values put IC 310 at the borderline between radio galaxies and blazars. The jet power estimated from observations of the large-scale radio jet is $L_{\rm j} = 2 \times 10^{42}$ erg s$^{-1}$, assuming that it contains only electrons, positrons, and magnetic fields in equipartition of their energy densities (section S1.3). For a radiative efficiency of 10%, the Doppler-boosted average luminosity of the jet emission amounts to $0.1\delta^4 L_{\rm j} \approx 5 \times 10^{43}$ erg s$^{-1}$, which is close to the one observed in very high-energy gamma rays. For $\delta$~4, the variability time scale in the co-moving frame of the jet, where it should be larger than $\Gamma_{\rm j}\Delta t_{\rm BH}$, is actually close to $\Delta t_{\rm BH}$ (Fig. 1). A very high value of the Doppler factor is required to avoid the absorption of the gamma rays due to interactions with low-energy synchrotron photons, inevitably co-produced with the gamma rays in the shock-in-jet scenario. The optical depth to pair creation by the gamma rays can be approximated by $\tau_{\gamma\gamma}(10\ {\rm TeV}) \sim 300(\delta/4)^{-6}(\Delta t/1\,{\rm min})^{-1}(L_{\rm syn}/10^{42}{\rm erg\,s^{-1}})$. Adopting a nonthermal infrared luminosity of ~1% of the gamma-ray luminosity during the flare, the emission region would be transparent to the emission of 10-TeV gamma rays only if $\delta \gtrsim 10$.

For the range of orientation angles inferred from radio observations, the Doppler factor is constrained to a value of $\delta < 6$ (Fig. 1). One can speculate whether the inner jet, corresponding to the unresolved radio core, bends into a just-right orientation angle to produce the needed high

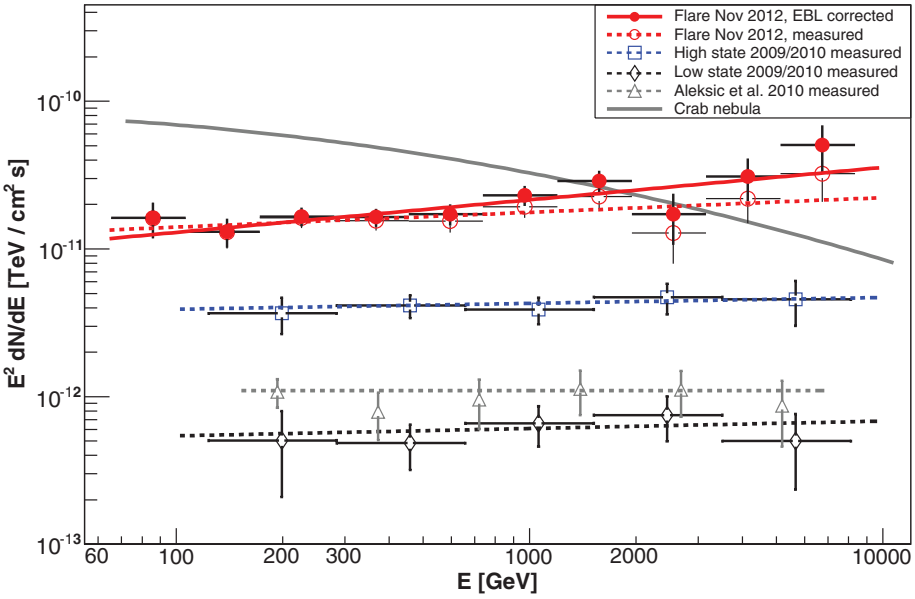


**Fig. 3. Average spectral energy distributions during the flare (red) along with previous measurements of IC 310 as observed by MAGIC.** We show the results from the high (blue, open squares) and low (black, open markers) states reported in (*28*) and the average results (gray triangles) from (*27*) for the whole period. The dashed lines show power-law fits to the measured spectra, and the solid line with solid circles depicts the spectrum corrected for absorption in the extragalactic background light. As a reference, the spectral power-law fit of the Crab Nebula observations from (*25*) is shown (gray, solid line). Vertical error bars show 1 SD statistical uncertainity. Because of the unfolding procedure, spectral points are correlated. Horizontal error bars show the energy binning.

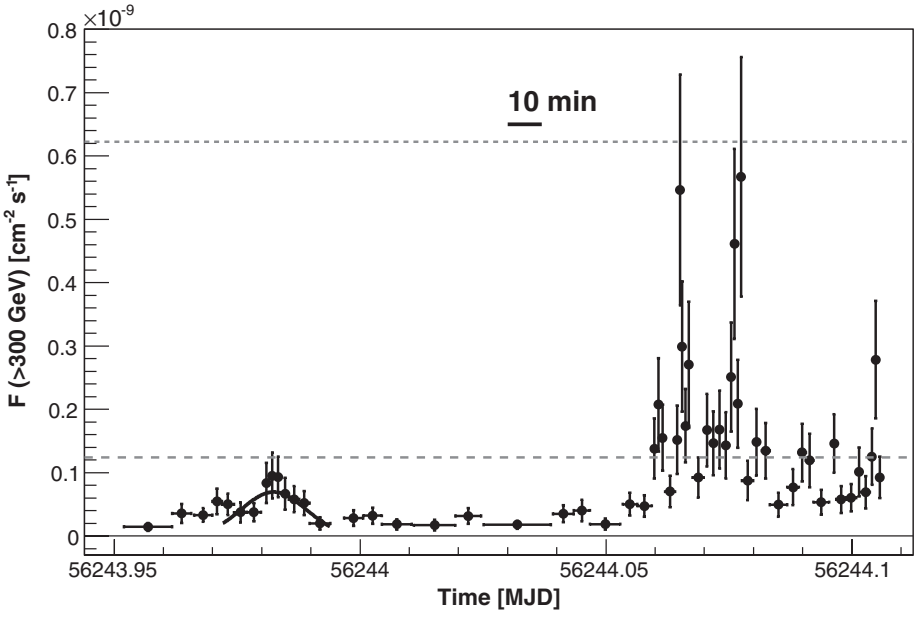


**Fig. 4. Light curve of IC 310 observed with the MAGIC telescopes on the night of 12/13 November 2012, above 300 GeV.** As a flux reference, the two gray lines indicate levels of 1 and 5 times the flux level of the Crab Nebula, respectively. The precursor flare (MJD 56243.972-56243.994) has been fitted with a Gaussian distribution. Vertical error bars show 1 SD statistical uncertainity. Horizontal error bars show the bin widths.

value of the Doppler factor (section S1.2). The probability of such an alignment seems to be rather low. Moreover, the observed radio jet does not show any signs of a perturbation of its flow direction on the parsec and kiloparsec scales. Because perturbations of the flow direction of the inner jet would later propagate to larger scales, major bends apparently never occurred in the past.

In summary, trying to interpret the data in the frame of the shock-in-jet model meets difficulties. Considering the role of time dilation renders a solution of this problem impossible for any value of $\Gamma_j$. Therefore, we conclude that the observations indicate a subhorizon-scale emission region of a different nature.

### Possible origins of subhorizon-scale variability

Substructures smaller than the event horizon scale emitting highly anisotropic radiation (to avoid pair absorption) seem to be responsible for the minute-scale flux variations. The possible explanations fall into three categories: (i) mini-jet structures within the jets (*33*); (ii) jet-cloud interactions, where the clouds may originate from stellar winds (*34*–*36*); and (iii) magnetospheric models (*37*–*41*), similar to those known from pulsar theory.

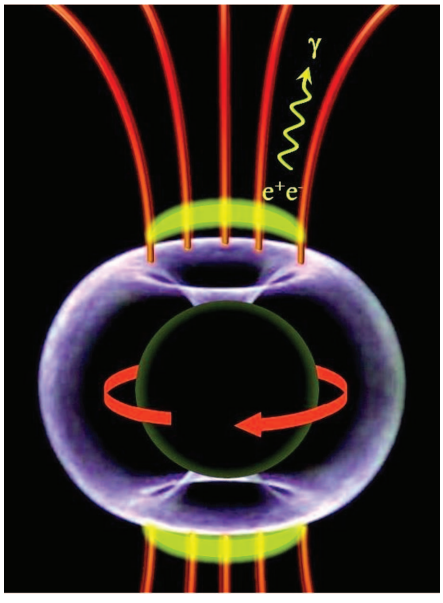


**Fig. 5. Scenario for the magnetospheric origin of the gamma rays:** A maximally rotating black hole with event horizon $r_g$ (black sphere) accretes plasma from the center of galaxy IC 310. In the apple-shaped ergosphere (blue) extending to $2r_g$ in the equatorial plane, Poynting flux is generated by the frame-dragging effect. The rotation of the black hole induces a charge-separated magnetosphere (red) with polar vacuum gap regions (yellow). In the gaps, the electric field of the magnetosphere has a component parallel to the magnetic field that is accelerating particles to ultrarelativistic energies. Inverse Compton scattering and copious pair production due to interactions with low-energy thermal photons from the plasma accreted by the black hole lead to the observed gamma rays.

According to the mini-jet model (i), plasmoids resulting from magnetic reconnection traveling down the jet with a relativistic speed are responsible for the minute-scale flux variations observed in blazars. The model could help to mitigate the constraints on the bulk Lorentz factor by introducing a larger effective bulk Lorentz factor for the plasmoids. The mechanism also predicts reconnection events from regions outside of the beaming cone $\sim\Gamma_j^{-1}$ that could explain the day-scale flares from the radio galaxy M87 invoking external radiation fields as a target for inverse Compton scattering (*33*). However, the off-axis mini-jet luminosity depends on $(\Gamma_j\theta)^{-8}$, and the jet power required for IC 310 is two orders of magnitude higher than the one estimated from radio observations (section S3.2). Thus, this model is challenged by the observed high luminosity in IC 310 during the flares.

Substructures smaller than the jet radius may also be introduced by considering interactions between clouds and the jet (ii). The original shock-in-jet model (*1*) considered this to be the main source of mass entrainment and predicted variability from the process. Recently, more elaborate work on the model has had some success in explaining the variability of M87 by proton-proton collisions due to the bombardment of clouds boiled off of red giants with protons in the jet (*36*). However, the model is linked to the cloud crossing time of the jet and the proton-proton cooling time, both of which far exceed the event horizon scale. Faster variability could be observed if the cloud gets destroyed, but a strong beaming effect would then be needed to explain the observed luminosities. In another variant, drift acceleration of particles along the trailing shock behind the stellar wind of a star interacting with the jet is considered. This might lead to an extremely anisotropic emission pattern. As mass-loosing stars sweep across the jet, passing magnetic field lines pointing to the observer, the postulated accelerated particle beams in their trails become visible for a short time. For IC 310, the emission would have to be confined to within an angle of $\alpha\sim10^{-5}$ rad to explain the observed variability time scale, requiring a very stable direction of the accelerated particle beams, at a large angle to the jet main thrust. Because two-fluid particle beams are prone to numerous plasma instabilities, the scenario relies on unphysical assumptions.

In magnetospheric models (iii), particle acceleration is assumed to be due to electric fields parallel to the magnetic fields. This mechanism is known to operate in the particle-starved magnetospheres of pulsars, but it could also operate in the magnetospheres anchored to the ergospheres of accreting black holes (Fig. 5). Electric fields can exist in vacuum gaps when the density of charge carriers is too low to warrant their shortcut. The critical charge density for the vacuum gaps is the so-called Goldreich-Julian charge density. Electron-positron pairs in excess of the Goldreich-Julian charge density can be produced thermally by photon-photon collisions in a hot accretion torus or corona surrounding the black hole. It has also been suggested that particles can be injected by the reconnection of twisted magnetic loops in the accretion flow (*39*). A depletion of charges from thermal pair production is expected to happen when the accretion rate becomes very low. In this late phase of their accretion history, supermassive black holes are expected to have spun up to maximal rotation. Black holes can sustain a Poynting flux jet by virtue of the Blandford-Znajek mechanism (*4*). Jet collimation takes place rather far away from the black hole at the scale of the light cylinder beyond $\sim10r_g$. Gaps could be located at various angles, with the jet axis corresponding to the polar and outer gaps in pulsar magnetospheres leading to fan beams at rather large angles with the jet axis. The gap emission must be highly variable, because gap height and seed particle content depend sensitively on plasma turbulence and accretion rate. For an accretion rate of $\dot{m}\sim10^{-4}$ (in units of the Eddington accretion rate) and maximal black hole rotation, the gap height in IC 310 is expected to be $h\sim0.2\,r_g$ (*40*), which is in line with the observations. Depending on the electron temperature and geometry of the radiatively inefficient accretion flow, its thermal cyclotron luminosity can be low enough to warrant the absence of pair creation attenuation in the spectrum of gamma rays. In this picture, the intermittent variability witnessed in IC 310 is due to a runaway effect. As particles accelerate to ultrahigh energies, electromagnetic cascades develop, multiplying the number of charge carriers until their current shortcuts the gap. The excess particles are then swept away with the jet flow, until the gap reappears.

Radio galaxies and blazars with very low accretion rates allow us to obtain a glimpse of the jet formation process near supermassive black holes. The subhorizon variability in combination with the results from direct imaging campaigns invite us to explore analogies with pulsars, where particle acceleration takes place in two stages. In the first stage, particle acceleration occurs in the gaps of a charge-separated magnetosphere anchored in the ergosphere of a rotating black hole, and in a second stage, particle acceleration occurs at shock waves in the force-free wind beyond the outer light cylinder.

### REFERENCES AND NOTES

1. R. D. Blandford, A. Königl, *Astrophys. J.* **232**, 34 (1979).
2. L. Maraschi, G. Ghisellini, A. Celotti, *Astrophys. J.* **397**, L5 (1992).
3. C. D. Dermer, R. Schlickeiser, *Astrophys. J.* **416**, 458 (1993).
4. R. D. Blandford, R. L. Znajek, *Mon. Not. R. Astron. Soc.* **179**, 433–456 (1977).
5. S. van Velzen, H. Falcke, *Astron. Astrophys.* **557**, L7 (2013).
6. A. P. Marscher, W. K. Gear, *Astrophys. J.* **298**, 114 (1985).
7. S. S. Doeleman *et al.*, *Science* **338**, 355–358 (2012).
8. I. Vovk, A. Neronov, *Astrophys. J.* **767**, 103 (2013).
9. J. Albert *et al.*, *Astrophys. J.* **685**, L23–L26 (2008).
10. A. Abramowski *et al.*, *Astrophys. J.* **746**, 151 (2012).
11. K. Gebhardt, J. Thomas, *Astrophys. J.* **700**, 1690–1701 (2009).
12. V. A. Acciari *et al.*, *Science* **325**, 444–448 (2009).
13. J. Albert *et al.*, *Astrophys. J.* **669**, 862–883 (2007).
14. F. Aharonian *et al.*, *Astrophys. J.* **664**, L71–L74 (2007).
15. M. C. Begelman, A. C. Fabian, M. J. Rees, *Mon. Not. R. Astron. Soc.* **384**, L19–L23 (2008).
16. In special relativity, the Lorentz and Doppler factors are defined as $\Gamma_j = (1-\beta^2)^{-1/2}$ and

$\delta = [\Gamma_j(1-\beta\cos\theta)]^{-1}$, respectively, where $\beta$ denotes the dimensionless shock velocity and $\theta$ the angle between the line of sight and the direction of the jet, ignoring the cosmological $(1+z)$ factor. The apparent bolometric luminosity differs from its isotropic co-moving–frame value by the factor $\delta^4$.
17. M. L. Lister *et al*., *Astron. J.* **138**, 1874–1892 (2009).
18. C. M. Urry, P. Padovani, M. Stickel, *Astrophys. J.* **382**, 501 (1991).
19. M. Lyutikov, M. Lister, *Astrophys. J.* **7**, 197–203 (2010).
20. G. Ghisellini, F. Tavecchio, *Mon. Not. R. Astron. Soc.* **386**, L28–L32 (2008).
21. D. Giannios, D. A. Uzdensky, M. C. Begelman, *Mon. Not. R. Astron. Soc.* **395**, L29–L33 (2009).
22. F. C. Michel, *Phys. Rev. Lett.* **23**, 247–249 (1969).
23. M. Lyutikov, *Mon. Not. R. Astron. Soc.* **396**, 1545–1552 (2009).
24. J. G. Kirk, I. Mochol, *Astrophys. J.* **729**, 104 (2011).
25. J. Aleksić *et al*., *Astropart. Phys.* **35**, 435–448 (2012).
26. A. Neronov, D. Semikov, I. Vovk, *Astron. Astrophys.* **519**, L6 (2010).
27. J. Aleksić *et al*., *Astrophys. J.* **723**, L207–L212 (2010).
28. J. Aleksić *et al*., *Astron. Astrophys.* **563**, A91 (2014).
29. K. Gültekin *et al*., *Astrophys. J.* **698**, 198–221 (2009).
30. D. B. McElroy, *Astrophys. J. S.* **100**, 105 (1995).
31. A. Merloni, S. Heinz, T. di Matteo, *Mon. Not. R. Astron. Soc.* **345**, 1057–1076 (2003).
32. M. Kadler *et al*., *Astron. Astrophys.* **538**, L1 (2012).
33. D. Giannios, D. A. Uzdensky, M. C. Begelman, *Mon. Not. R. Astron. Soc.* **402**, 1649–1656 (2010).
34. W. Bednarek, R. J. Protheroe, *Mon. Not. R. Astron. Soc.* **287**, L9–L13 (1997).
35. M. V. Barkov, F. A. Aharonian, V. Bosch-Ramon, *Astrophys. J.* **724**, 1517–1523 (2010).
36. M. V. Barkov, V. Bosch-Ramon, F. A. Aharonian, *Astrophys. J.* **755**, 170 (2012).
37. F. M. Rieger, K. Mannheim, *Astron. Astrophys.* **353**, 473 (2000).
38. A. Neronov, F. A. Aharonian, *Astrophys. J.* **671**, 85–96 (2007).
39. A. Y. Neronov, D. V. Semikoz, I. I. Tkachev, *New J. Phys.* **11**, 065015 (2009).
40. A. Levinson, F. Rieger, *Astrophys. J.* **730**, 123 (2011).
41. V. S. Beskin, Y. N. Istomin, V. I. Parev, *SOVAST* **36**, 642 (1992).

### ACKNOWLEDGMENTS

We thank the Instituto de Astrofisica de Canarias for the excellent working conditions at the Observatorio del Roque de los Muchachos in La Palma. The support of the German BMBF and MPG, the Italian INFN, the Swiss National Fund SNF, and the Spanish MICINN is gratefully acknowledged. This work was also supported by the CPAN CSD2007-00042 and MultiDark CSD2009-00064 projects of the Spanish Consolider-Ingenio 2010 program, by grant 127740 of the Academy of Finland, by the DFG Cluster of Excellence "Origin and Structure of the Universe", by the Croatian Science Foundation (HrZZ) Projects 09/176, by the University of Rijeka Project 13.12.1.3.02, by the DFG Collaborative Research Centers SFB823/C4 and SFB876/C3, and by the Polish MNiSzW grant 745/N-HESS-MAGIC/2010/0. We thank also the support by DFG WI 1860/10-1. J. S. was supported by ERDF and the Spanish MINECO through FPA2012-39502 and JCI-2011-10019 grants. E. R. was partially supported by the Spanish MINECO projects AYA2009-13036-C02-02 and AYA2012-38491-C02-01 and by the Generalitat Valenciana project PROMETEO/2009/104, as well as by the COST MP0905 action 'Black Holes in a Violent Universe.' The European VLBI Network is a joint facility of European, Chinese, South African and other radio astronomy institutes funded by their national research councils. The research leading to these results has received funding from the European Commission Seventh Framework Programme (FP/2007-2013) under grant agreement No. 283393 (RadioNet3). The MAGIC data are archived in the data center at the Port dInformació Cientfica (PIC) in Barcelona. The EVN data are available at the Data Archive at the Joint Institute for VLBI in Europe (JIVE).

### SUPPLEMENTARY MATERIALS

www.sciencemag.org/content/346/6213/1080/suppl/DC1
Materials and Methods
Figs. S1 to S5
Tables S1 and S2
References (*42*–*69*)

16 May 2014; accepted 23 October 2014
10.1126/science.1256183

PLANT SCIENCE

# Biosynthesis, regulation, and domestication of bitterness in cucumber

**Yi Shang,[1,2]* Yongshuo Ma,[1,3]* Yuan Zhou,[1,4]* Huimin Zhang,[1,3]* Lixin Duan,[5] Huiming Chen,[6] Jianguo Zeng,[4] Qian Zhou,[1] Shenhao Wang,[1] Wenjia Gu,[1,7] Min Liu,[1,3] Jinwei Ren,[8] Xingfang Gu,[1] Shengping Zhang,[1] Ye Wang,[1] Ken Yasukawa,[9] Harro J. Bouwmeester,[10] Xiaoquan Qi,[5] Zhonghua Zhang,[1] William J. Lucas,[11] Sanwen Huang[1,2]†**

**Cucurbitacins are triterpenoids that confer a bitter taste in cucurbits such as cucumber, melon, watermelon, squash, and pumpkin. These compounds discourage most pests on the plant and have also been shown to have antitumor properties. With genomics and biochemistry, we identified nine cucumber genes in the pathway for biosynthesis of cucurbitacin C and elucidated four catalytic steps. We discovered transcription factors *Bl* (*Bitter leaf*) and *Bt* (*Bitter fruit*) that regulate this pathway in leaves and fruits, respectively. Traces in genomic signatures indicated that selection imposed on *Bt* during domestication led to derivation of nonbitter cucurbits from their bitter ancestors.**

Plant specialized metabolites play essential roles in mediating interactions between the plant and its environment and constitute a valuable resource in discovery of economically important molecules. In the plant family *Cucurbitaceae*, a group of highly oxygenated tetracyclic and bitter triterpenes, the cucurbitacins, mediated the coevolution between cucurbits and herbivores. They serve either as protectants against generalists or feeding attractants to specialists (*1*–*3*). Widely consumed as vegetables and fruits, cucurbits were domesticated from their wild ancestors that had extremely bitter fruits. Drought and temperature stress can increase the bitterness in certain domesticated cultivars, which can affect fruit quality and marketability. Molecular insights into the occurrence and domestication of bitterness in cucurbits remain largely unknown.

Despite their presence in fruits as a negative agricultural taste, cucurbitacins have for centuries been exploited for anti-inflammatory and hepatoprotective activities, in the form of traditional herbal medicines (*4*, *5*). Bitter fruits and leaves of wild cucurbit plants have been used as a purgative and emetic in India (*6*). The bitter fruit stem of melon (in Chinese, "gua di") is prescribed as a traditional hepatoprotective medicine whose effect and usage were well documented in *Ben Cao Gang Mu*, the Chinese Encyclopedia of Botany and Medicines composed by the Ming Dynasty physician Li Shi-Zhen in 1590 CE. Recent studies revealed that cucurbitacins can cause cell-cycle arrest, apoptosis, and growth suppression of cancer cells through the specific inhibition of the Janus kinase–signal transducers and activators of transcription (JAK-STAT) pathway (*7*, *8*). At present, their low concentrations in plants and nonspecific cytotoxicity limit their pharmaceutical applications.

To date, plant metabolic diversification studies (*9*, *10*), as well as recently reported gene clusters in plants [reviewed in (*11*)], indicate that clustering of functionally-related genes for the biosynthesis of secondary metabolites may well be a common feature of plant genomes. In cucumber, two interacting Mendelian loci were reported to control the bitterness, conferred predominantly by cucurbitacin C (CuC) (*3*, *12*). The *Bi* gene (*1*) confers bitterness to the entire plant and is genetically associated with an operon-like gene cluster (*13*), similar to the gene cluster involved in thalianol biosynthesis in *Arabidopsis* (*14*). Fruit bitterness requires both *Bi* and the dominant *Bt* (*Bitter fruit*) gene. Nonbitterness of cultivated cucumber fruit is conferred by *bt*, an allele selected during domestication as indicated by population genomics (*15*). Exploiting these genetic clues, here we report the discovery of 11 genes involved in the biosynthesis, regulation, and domestication of cucumber bitterness.

## First committed step in CuC biosynthesis

To identify genetic variants associated with *Bi*, a genome-wide association study was performed

[1]Institute of Vegetables and Flowers, Chinese Academy of Agricultural Sciences, Key Laboratory of Biology and Genetic Improvement of Horticultural Crops of the Ministry of Agriculture, Sino-Dutch Joint Laboratory of Horticultural Genomics, Beijing 100081, China. [2]Agricultural Genomic Institute at Shenzhen, Chinese Academy of Agricultural Sciences, Shenzhen 518124, China. [3]College of Life Sciences, Nanjing Agricultural University, Nanjing 210095, China. [4]Horticulture and Landscape College, Hunan Agricultural University, National Chinese Medicinal Herbs Technology Center, Changsha 410128, China. [5]Institute of Botany, Chinese Academy of Sciences, Beijing 100093, China. [6]Hunan Vegetable Research Institute, Hunan Academy of Agricultural Sciences, Changsha 410125, China. [7]College of Life Sciences, Wuhan University, Wuhan 430072, China. [8]Institute of Microbiology, Chinese Academy of Sciences, Beijing 100190, China. [9]School of Pharmacy, Nihon University, Tokyo 101-8308, Japan. [10]Laboratory of Plant Physiology, Wageningen University, Wageningen 6700, Netherlands. [11]Department of Plant Biology, College of Biological Sciences, University of California, Davis, CA 95616, USA.
*These authors contributed equally to this work. **†Corresponding author. E-mail: huangsanwen@caas.cn**

# Black hole lightning due to particle acceleration at subhorizon scales

J. Aleksic *et al.*

*Science* **346**, 1080 (2014);
DOI: 10.1126/science.1256183